NARROWBAND DELAY ESTIMATION FOR THALAMOCORTICAL EPILEPTIC SEIZURE PATHWAYS

David L. Sherman*, Yien Che Tsai*, Lisa Ann Rossell**,
Marek A. Mirski** and Nitish V. Thakor*

Departments of Biomedical Engineering* and Anesthesiology and Critical Care Medicine**
Johns Hopkins University School of Medicine
720 Rutland Avenue
Baltimore, MD 21205, USA

ABSTRACT

Time series analysis applications of eigenstructure algorithms focus on temporal frequency estimation . We show that the *ESPRIT* algorithm can also be applied to simple phase delays for sinusoids. We show that a time delay data model can be rendered in the *ESPRIT* matrix pencil structure. The *PRO-ESPRIT* formulation can be then utilized to solve for phase delays among sinusoids. An application area for this algorithm is the estimation of short time delays for low frequency sinusoids comprising EEG (electroencephalographic) recordings derived from different neural sites during epileptic seizure activity.

1. INTRODUCTION

Array signal processing algorithms utilizing eigenstructure models have shown to provide robust frequency estimation of time series data [6, 9, 12]. Sinusoidal parametrization offers the advantage of high resolution coupled with time domain data processing which isolates noise contributions resulting in a higher SNR environment. The *ESPRIT* algorithm of Paulraj, Roy and Kailath [6, 7, 8] provides frequency estimation performance through the exploitation of invariant structure of uniformly sampled data [6, 12]. This algorithm can furnish sinusoidal series time delay estimates as it does frequency and angle-of-arrival estimation [9,12].

As has been illustrated in previous accounts [9], these array processing techniques often find widespread applicability in neural signal processing situations. It offers a compact representation of aberrant highly synchronized oscillatory behavior in the central nervous system. In the current scenario we chose to study the delay relationships of low frequency sinusoids between electroencephalogram (EEG) electrode recording sites during chemically-induced epileptic seizures in animals models. The tracking of EEG signals during epileptic seizures is critical for the identification of neural pathways active in the propagation of paroxysmal electrical activity. The development of robust and reliable time delay estimation (TDE) algorithms for epileptic seizure pathway localization is of intense, current interest [10]. Studies in our laboratories have focused on identifying the involvement of subcortical centers in the propagation of generalized seizures in the rat. The use of a variety of neurophysiological techniques have identified the anterior thalamus (AN), a collection of specialized nerve cells in the subcortical region of the brain, as a functional relay for generalized epileptic seizures [1, 2, 3, 4]. EEG recordings from cortex (CTX) as well as other subcortical sites such as hippocampus (HPC) have been made for electrical signal confirmation of seizure pathways. Ordinary and partial coherence studies have indicated that a narrow range of low (0-6 Hz) frequencies between AN and cortex is uniformly high in coherence. Reliably high coherences ($\gamma(f) > 0.8$) are often found in this baseband frequency range. This is within the spike repetition rate range for several models of spike-wave epilepsies [5].

Since we would like to establish finite non-zero time delays between AN and CTX, we can capitalize on the results of exploratory data analysis and calculate time delays *within a purely narrowband region of the frequency spectrum.* Within this low frequency portion of the spectrum, we can represent signals at CTX and AN by simple delayed sinusoids. The *PRO-ESPRIT* formulation of Zoltowski and Stavrinides [8, 9 12] is the *ESPRIT* technique utilized. *PRO-ESPRIT* offers robust results with few data realizations. This method can handle singular forms through a systemic transition from signal or data matrices to noise-free or "cleaned" correlation matrices. Once the number of sinusoids is known, the correlation matrices can be reduced to the full rank signal information matrix at the core rotations level. The eigenvalues of this matrix are the GEs (generalized eigenvalues) of the singular data matrices. These contain the necessary phase information dealing with delays. *PRO-ESPRIT* also provides a method for associating frequency estimates with corresponding phase delays factors. In sections 1 and 2 we show ESPRIT time delay formulation and its solution. Through computer

0-7803-2431-5/95 $4.00

simulations and real data analysis, we show the practical use of this method in sections 3 and 4, respectively.

1. SIGNAL MODEL

A collection of D sinusoidal signals, $s_i(t)$, for $i = 1,\ldots D$, with fixed amplitudes plus additive stationary white noise, $n_x(t)$, comprises signal, $x(t)$. At different observation times or snapshot, $k, k = 1,\ldots N$, a signal of length M is recorded. The signal representation is

$$x_k(t) = \sum_{i=1}^{D} a_{k,i} s_i(t) + n_{k,1}(t) \qquad (1)$$

$$= \sum_{i=1}^{D} a_{k,i} \exp(j\omega_i t) + n_{k,1}(t).$$

The amplitude coefficient, $a_k = A_i \exp(j\theta_{k,i})$ consists of a random phase term, $\exp(j\theta_{k,i})$, as well as amplitude terms, A_i. We assume that the amplitude terms are constant from observation interval to observation interval. Another assumption is that the sinusoids are uncorrelated so that all k,

$$\theta_{k,i} \neq m\theta_{k,j}$$

holds for $i = 1,\ldots D$; $j = 1,\ldots D$ and i ≠ j and m is a real constant. The noise is considered to be uncorrelated from one observation interval to the next.

The signal from x is delayed and appears at another recording site, y, with its own additive white noise source, $n_2(t)$, which is uncorrelated with the noise at x. At site y each sinusoid term is delayed a fixed angular quantity, ϕ_i so that the signal appears as

$$y_k(t) = \sum_{i=1}^{D} a_{k,i} s_i(t - T_i) + n_{k,2}(t) \qquad (2)$$

$$= \sum_{i=1}^{D} a_{k,i} \exp(j\phi_i) \exp(j\omega_i t) + n_{k,2}(t)$$

The relationship between temporal and angular delay is simply $T_i = \phi_i / \omega_i$. We assume that delays for each sinusoid are independent of one another so that the traditional linear delay hypothesis need not be followed.

Each signal captured during a particular observation interval can be rewritten as an Mx1 vector

$$\mathbf{x}(k) = \left[x_k(1) \;\; x_k(2) \;\; \ldots \;\; x_k(M)\right]^T.$$

(A similar form exists for $\mathbf{y}(k)$). All of N individual vectors, $\mathbf{x}(1), \mathbf{x}(2), \ldots \mathbf{x}(k)$, can be grouped to form a MxN data matrix $\mathbf{X}$

$$\mathbf{X} = \left[\mathbf{x}(1)\mathbf{x}(2)\cdots\mathbf{x}(N)\right]$$

These data matrices can be decomposed into

$$\mathbf{X} = \mathbf{SA} + \mathbf{N}_x = \sum_{i=1}^{D} \mathbf{s}_i \mathbf{a}_i^T + \mathbf{N}_x \qquad (3a)$$

$$\mathbf{Y} = \mathbf{S\Phi A} + \mathbf{N}_y = \sum_{i=1}^{D} \phi_{ii} \mathbf{s}_i \mathbf{a}_i^T + \mathbf{N}_y \qquad (3b)$$

where $\Phi = diag\left[\exp(j\phi_1) \;\; \exp(j\phi_2) \;\cdots\; \exp(j\phi_D)\right]$ and

$$\mathbf{S} = \left[\mathbf{s}_1 \;\; \mathbf{s}_2 \;\cdots\; \mathbf{s}_D\right]$$

$$\mathbf{s}_i^T = \left[1 \;\; \exp(j\omega_i) \;\; \exp(j2\omega_i) \;\cdots\; \exp(j(M-1)\omega_i\right]$$

$$\mathbf{A} = \left[\mathbf{a}_1 \;\; \mathbf{a}_2 \;\cdots\; \mathbf{a}_D\right]$$

$$\mathbf{a}_i = \left[A\exp(j\theta_{i,1}) \;\; A\exp(j\theta_{i,2}) \;\ldots\; A\exp(j\theta_{i,N})\right]$$

Examining the noise-free data matrices we can easily see that the data matrices have the necessary *ESPRIT* matrix pencil structure at this juncture, namely

$$\mathbf{Y}_D - \lambda\mathbf{X}_D = \sum_{i=1}^{D} (\phi_i - \lambda)\mathbf{s}_i \mathbf{a}_i^T \qquad (4)$$

Data vectors in matrix **Y differ only** by those in matrix **X** by an angular displacement or phase delay, $\phi_i, i = 1,\ldots D$. When $\lambda = \phi_i$, the rank of the pencil drops by one. Following [7] the delays are the generalized eigenvalues of the matrix pencil, $\{\mathbf{Y}, \mathbf{X}\}$. It is important to note that we have not restricted the GEVs to the unit circle. Without any gain compensation, the GEVs may deviate from the unit circle.

2. SOLVING FOR THE GENERALIZED EIGENVALUES IN A DELAY MODEL

Following singular value decomposition (SVD) of the **X** data matrix we have

$$\frac{1}{\sqrt{N}}\mathbf{X}_D = \mathbf{U}_x^D \Sigma_x^D \mathbf{V}_x^{DH} = \sum_{i=1}^{D} \sigma_{x_i} \mathbf{u}_{x_i} \mathbf{v}_{x_i}^H \qquad (5)$$

where $\mathbf{X}_D$ is the noise-free data matrix weighted by the variance stabilizing constant, $1/\sqrt{N}$. Here we include only those left and right singular vectors with nonzero singular values and signify this by the use of the D subscript. In [12] we see that the matrix pencil, $\mathbf{Y} - \lambda\mathbf{X}$, can be written in terms of the components of (5), namely

$$\mathbf{Y}_D - \lambda\mathbf{X}_D = \mathbf{U}_x{}^D \mathbf{U}_x{}^{DH} \mathbf{Y}_D \mathbf{V}_x{}^D \mathbf{V}_x{}^{DH} - \lambda \mathbf{U}_x{}^{DH} \Sigma_x{}^D \mathbf{V}_x{}^D \qquad (6)$$

where we exploit the orthogonality of left and right singular vectors. Ultimately the GEs for this matrix arise from the core information matrix (CIM) rendition derived from the proof in [12] and equivalent to the CIM in [8].

$$\mathbf{Y}_D - \lambda\mathbf{X}_D = \mathbf{U}_x^D \Sigma_x^D \left\{ \Sigma_x^{D^{-1}} \mathbf{U}_x^{DH} \mathbf{Y}_D \mathbf{X}_D{}^H \mathbf{U}_x^D \Sigma_x^{D^{-1}} - \lambda \mathbf{I}^D \right\} \mathbf{V}_x^{DH}. \qquad (7)$$

An eigenvalue/eigenvector decomposition (EVD) of the CIM or $\Psi = \Sigma_x^{D^{-1}} \mathbf{U}_x^{DH} \mathbf{Y}_D \mathbf{X}_D{}^H \mathbf{U}_x^D \Sigma_x^{D^{-1}}$ gives the GEVs that we need to find the phase delays for the various sinusoids.

As we do not have access to noisefree SVDs of the data matrices, we deal with quantities derived from the cross-correlation matrix,

$$\mathbf{C}_{yx} = \frac{1}{N}\sum_{k=1}^{N} \mathbf{y}_k \mathbf{x}_k^{\mathrm{H}} = \frac{1}{N}\mathbf{Y}_D \mathbf{X}_D{}^H, \quad (8)$$

and the EVD of the "clean" autocorrelation matrix,

$$\mathbf{C}_{xx} = \frac{1}{N}\sum_{i=1}^{N} \mathbf{x}_k \mathbf{x}_k{}^H = \frac{1}{N}\mathbf{X}_D \mathbf{X}_D{}^H = \mathbf{U}_x^D \Sigma_x^{D^2} \mathbf{U}_x^D \quad (9)$$

Here noise contributions have been removed from the D largest eigenalues.

We also need to associate a particular GE or phase angle with its corresponding frequency component. As in [12] we note that the orthogonality of right singular vector of the data matrix pencil $\{\mathbf{Y} - \lambda\mathbf{X}\}\mathbf{r}_j = 0$ guarantees that

$$\mathbf{X}\mathbf{r}_j = c\mathbf{s}_j = \mathbf{U}_x^D \Sigma_x^D \beta_j \quad (10)$$

where β_j is the jth eigenvector of Ψ and c is a constant. Since $\mathbf{s}_j$ has a Vandermonde structure, specific frequency information can be extracted by first normalizing $c\mathbf{s}_j$ by its first element, c, to arrive at $\mathbf{s}_j$. At this point the frequency associated with the jth GE is proportional to the argument of any element of $\mathbf{s}_j$.

3. SIMULATION: COHERENCE EFFECTS

In order to test the performance of the algorithm, the accuracy of phase delay estimation was conducted on a computer using MATLAB with varying levels of coherence. Unity amplitude complex sinsusoids at frequencies, $f_1 = 0.11$ & $f_2 = 0.18$ comprise the signal $x(t)$. Delayed versions of each signal comprise a portion of the signal at y with phase delays of 0.691 and 1.508 radians, respectively. The signal at y also contained a signal at frequency f_2 fwith random phase uncorrelated with either of the delayed signals. The power of this signal was varied and P_f, the fraction of correlated signal energy to total power at y for the signals at f_2 was calculated according to $P_f = A^2/(A^2 + B^2)$ where A and B are the amplitudes of correlated and uncorrelated sinusoids, respectively. Data for both $x(t)$ and $y(t)$ was free of noise for this test.

Table 1: STANDARD DEVIATION OF PHASE DELAY AS A FUNCTION OF CORRELATED SIGNAL FRACTION (in fractions of 2π)

Power Fraction	Number of Observations		
	10	20	40
0.990	0.0037	0.0026	0.0019
0.962	0.0066	0.0047	0.0034
0.862	0.0134	0.0092	0.0075
0.735	0.0234	0.0148	0.0115
0.610	0.0272	0.0195	0.0131
0.50	0.0392	0.0242	0.0165
0.310	0.0644	0. 0418	0.0240
0.20	0.0821	0.0538	0.0401

Simulations consisted of 100 trials containing N=10, 20 or 40 observations or "snapshots" each. One observation consisted of 10 data points. Kronecker products forming 10x10 correlation matrices were used. For the purposes of angle estimation the two largest eigenvalues and their respective eigenvectors were used from $\mathbf{C}_{xx}$ for generating Ψ. Standard deviations of phase estimates were calculated and presented in Table 1. There is an decrease in variance as expected with an increase in the number of observations. Likewise as the uncorrelated power increases, the variation in phase delay increases as well. This shows that coherence efffects determine the accuracy of the phase estimation.

4. DELAYS IN EXPERIMENTAL DATA

Experiments were undertaken which induced seizures in rats. The model for generalized seizures used pentylenetrazol (PTZ) as the agent for seizure induction. Electrodes were placed epidurally for cortical recordings with depth electrodes in (HPC), AN as well as posterior thalamus (PT). The protocol for electrode placement as well as animal care and experimentation is described elsewhere [4].

During the experiment 4 channels of EEG are recorded continuously using a Grass amplifier. Data was sampled at 500 Hz. To prepare the data it was filtered and downsampled to 62.5 Hz. The data was filtered using a lowpass Park-McClennan filter with a cutoff of 6 Hz. The analytic signal was formed after taking the Hilbert transform of long data segments. Filtering restricted the time series to having mostly a single dominant sinusoid at the repetitiion frequency. Segments of EEG during clonic episodes were analyzed from CTX, AN and HPC. Examples of data from AN and Cortex are shown in Figs. 1 and 2, respectively.

The algorithm was implemented over several 2 second epochs using 120 observation intervals each 10 pts. long. New intervals began after one point increments according to [12] so that overlap is 119 data points. The overlap between epochs was 50% or one second. Model order was set to 1. GE estimation for phase delay was made using the eigenvalues of the CIM in (7). Frequency estimates for this single dominant sinusoid and its corresponding GE was made using the MUSIC algorithm and the eigenvectors from $x(t)$ and $y(t)$. The frequency estimate for the respective GE must be less than 6 Hz. Also to be considered a valid phase delay estimate, the corresponding frequency estimates for $x(t)$ and $y(t)$ must

not differ by more than $2\Delta_f$ where $\Delta_f = 0.3125$ Hz so that widely varying frequency estimates are rejected.

In Fig. 3 we can see that for one of the animals the delay actually drifts over time and begins to shorten. Delays start out as 100 ms and decrease to nearly 60 ms.

Ultimately, the delay for communication between subcortical centers is shorter by about 1/4. In the same animal delays between HPC and AN average over two clonic episodes to 2.5 and 11.6 ms with AN leading.

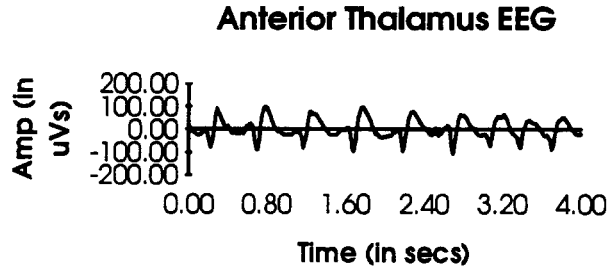

Fig. 1. Example of Seizure EEG from AN

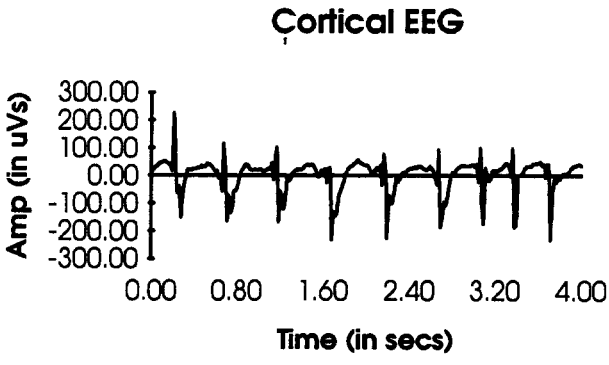

Fig. 2 Example of Cortical EEG

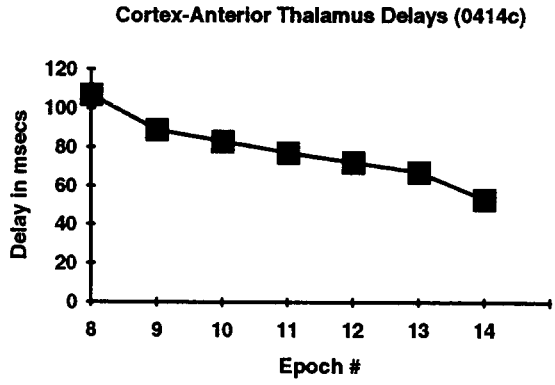

Fig.3 Drift in Cortical-Anterior Thalamus Delays During a Clonic Episode. Positive Delays Indicate that Cortex is Leading

This series of short delays may illustrate the ultimate practicality of these methods, namely the calculation of extremely short time delays that are evident for groups of neurons (nuclei) that are in close proximity to one another.

5. CONCLUSIONS

The use of eigenstructure techniques is a versatile tool in the analysis of seizure pathways. Parametric modeling of seizure events affords us the opportunity to examine very short sinusoidal delay during highly correlated seizure activity between recording sites within a particular frequency band.

6. REFERENCES

1. M.A. Mirski and J.A. Ferrendelli, "Interruption of the Mamillothalamic Tracts Prevents Seizures in Guinea Pigs." *Science,* 226, p 72-74, 1984.

2. M.A. Mirski and J.A. Ferrendelli, "Selective Metabolic Activation of Mammilary Bodies and Their Connections During Ethoximide-Induced Suppression of Pentylenetetrazol Seizures." *Epilepsia,* 27, p. 194-203, 1986.

3. M.A. Mirski and J.A. Ferrendelli, "Anterior Thalamic Mediation of Generalized Pentylenetetrazol Seizures." *Brain Research,* 397, p. 377-380, 1986.

4. D.L. Sherman, L.A. Rossell, Y-C Tsai, A.Kolandaivelu, E. Lancaster, N.V. Thakor, M.A. Mirski, "Confirming a Thalamocortical Seizure Pathway Using Signal Analysis." (submission pending, *IEEE Trans. BME*)

5. E.M. Marcus, "Experimental Models of Petit Mal Epilepsy," in D.M. Purpura, et al., in *Experimental Models of Epilepsy*, New York: Raven, 1972

6 R. Roy, A. Paulraj, and T. Kailath, "ESPRIT--A Subspace Rotation Approach to Estimation of Cisoids in Noise," *IEEE Trans. ASSP*, vol. ASSP-34, p. 1340-1342, 1986.

7 R. Roy, and T. Kailath, "ESPRIT-- Estimation of Signal Parameters Via Rotational Invariance Techniques," *IEEE Trans. ASSP*, vol. ASSP-37, p. 984-996, 1989.

8. M.D. Zoltowski and D. Stavrinides, "Sensor Array Signal Processing Via a Procrustes Rotations Based Eigenanalysis of the ESPRIT Data Pencil," *IEEE Trans. ASSP*, vol. ASSP-37, p. 832-861, 1989.

9. D.L Sherman and M.D. Zoltowski, "Matrix-Based Higher Order Spectral Analysis for Three-Wave Coupling, *IEEE Trans. SP.*, 42, p. 332-348, 1994.

10. P.Y Ktonas, "Automated EEG Analysis: Applications in Epilepsy." *Neuroengineering*, N.V. Thakor, Ed. (to appear)

11. M. Goldburg and R. Roy, "Application of ESPRIT to Parameter Estimation from Uniformly Sampled Data," Proc. Intl. Conf. Acoust. Speech Sig. Proc., Albuquerque, 1990.

12. M.D. Zoltowski and C.P. Mathews, "Real-Time Frequency and 2-D Angle Estimation with Sub-Nyquist Spatio-Temporal Sampling. *IEEE Trans. SP.*, 42, p. 2781-2794, 1994. (see also Proc. ICASSP-93)